

## IN SEARCH OF THE BOX ANOMALY BY STUDYING THE DECAY $\eta \rightarrow \pi^+ \pi^- \gamma$

---

**Daniel Lersch**<sup>\*†</sup>

*IKP1 Forschungszentrum Jülich, Germany*

*E-mail: [d.lersch@fz-juelich.de](mailto:d.lersch@fz-juelich.de)*

The following article deals with the analysis of the charged meson decay channel  $\eta \rightarrow \pi^+ \pi^- \gamma$ , as the decay mode of this channel, at the chiral limit, is described by the box anomaly. The mesons were produced in the reaction  $pp \rightarrow pp\eta$  at a proton beam momentum of  $1.4 \frac{\text{GeV}}{c}$ . The measurement was performed at the WASA facility at COSY. First results will show how the channel of interest is selected, using techniques like a kinematic fit and how the remaining background is determined.

*Xth Quark Confinement and the Hadron Spectrum,*

*October 8-12, 2012*

*TUM Campus Garching, Munich, Germany*

---

<sup>\*</sup>Speaker.

<sup>†</sup>For the WASA-at-COSY-Collaboration

## 1. Introduction & motivation

The decay channel  $\eta \rightarrow \pi^+\pi^-\gamma$  provides the opportunity to study QCD anomalies at the chiral limit. The decay width and the shape of the  $E_\gamma$ -distribution of this channel are sensitive to the

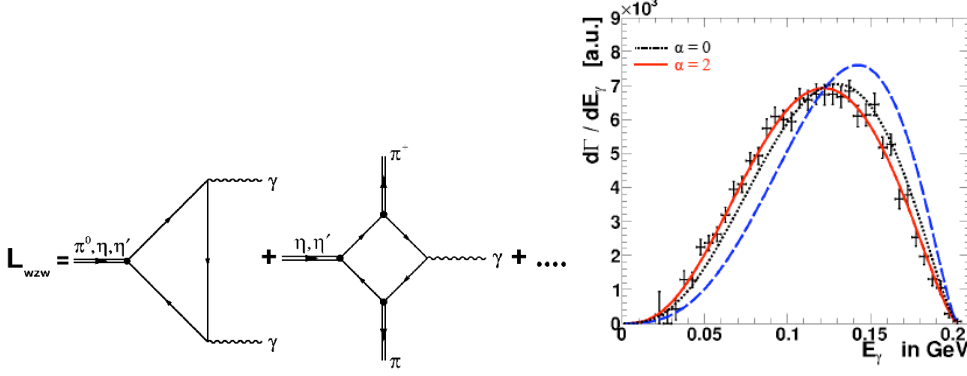


**Figure 1:** Left: Wess-Zumino-Witten-Lagrangian ( $L_{WZW}$ ) including the triangle anomaly (first) and box anomaly (second) term. [1]. Right: Measured  $E_\gamma$  distribution for the reaction:  $pd \rightarrow {}^3\text{He}[\eta \rightarrow \pi^+\pi^-\gamma]$  [4]. The measurement has been performed with high statistics and was fully efficiency corrected. The measured  $E_\gamma$  distribution is described by multiplying the simplest gauge invariant matrix element (blue curve) with a form factor (dashed and red curve) which depends on a single parameter  $\alpha$ . [5]

box anomaly term which is part of the Wess-Zumino-Witten-Lagrangian (see Fig. 1). However, the theoretically predicted decay width and  $E_\gamma$ -distribution do not agree with the experimental results, if final state interactions are not included by unitarized extensions of the  $L_{WZW}$ . The experimental observables for testing these extensions are (i) the branching ratio [2, 3] or (ii) the distribution of the single photon energy [3]. A recent measurement of the photon energy (see Fig. 1) with the WASA detector can be found in [4].

The aim of this work is to measure the branching ratio and the single photon energy distribution in one experiment using the reaction:  $pp \rightarrow pp[\eta \rightarrow \pi^+\pi^-\gamma]$ . The data have been acquired during 20 weeks in spring 2010 and 2012. At least  $10^6$   $\eta \rightarrow \pi^+\pi^-\gamma$  events are expected.

The WASA detector (see Fig. 2) is divided into two parts: the forward detector and the central detector.

Scattered projectiles or charged recoil particles are identified in the forward detector, a tracking detector with a set of range hodoscopes, which uses the  $\frac{dE}{E}$ -method for particle identification and reconstruction.

Decay products are measured with the central detector. Charged particles are identified by inspecting the deposited energy as function of the momentum as measured with a tracking device in a magnetic field. Neutral particles are detected in the calorimeter.

## 2. Data analysis

The recent analysis focusses on reconstructing  $\eta \rightarrow \pi^+\pi^-\gamma$ -events, but also investigates the channel  $\eta \rightarrow \pi^+\pi^-\pi^0$ . This channel is important for determining the relative branching ratio  $\frac{\Gamma_{\eta \rightarrow \pi^+\pi^-\gamma}}{\Gamma_{\eta \rightarrow \pi^+\pi^-\pi^0}}$  and contributes to the background of  $\eta \rightarrow \pi^+\pi^-\gamma$ . The  $\pi^0$  is also used for monitoring the calorimeter calibration. 1.2% of the total 2010 data have been analysed with the recent analysis

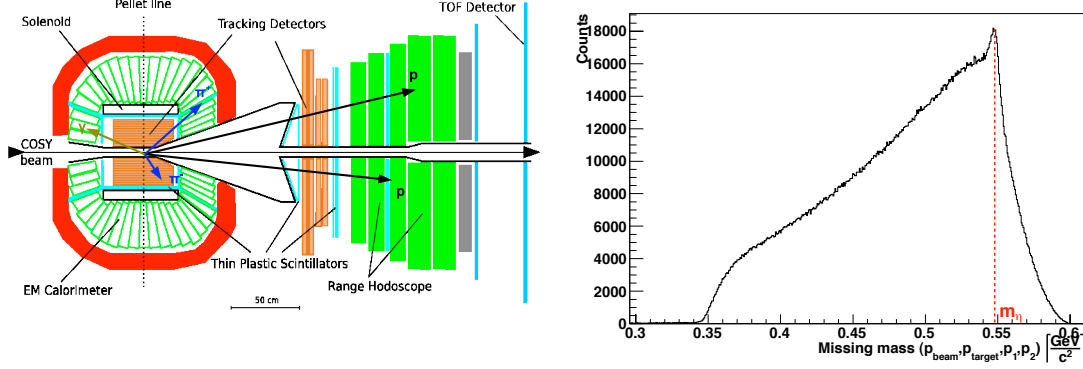


**Figure 2:** Left: Schematic drawing of the WASA detector. Right: Missing mass deduced from the initial state and the two final state protons. The red line indicates the  $\eta$ -mass at  $0.548 \text{ GeV}/c^2$ . This spectrum is obtained after proton reconstruction in the forward detector.

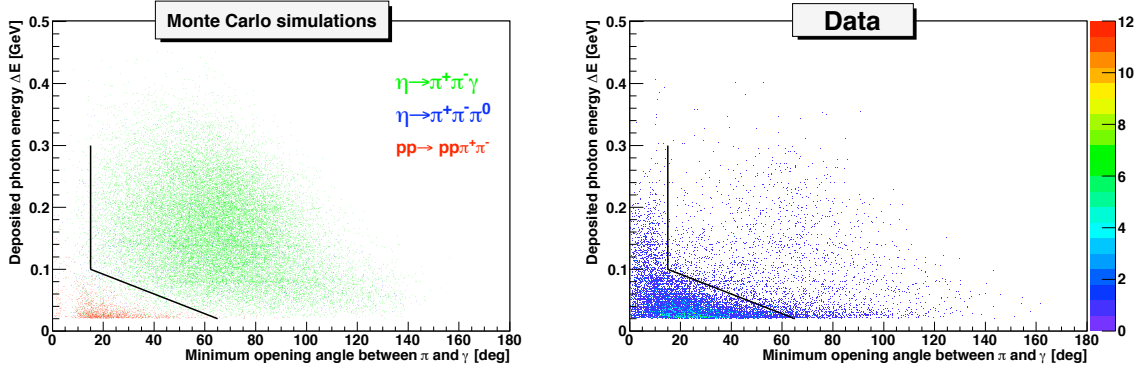


**Figure 3:** Plot of the photon energy as function of the minimum angle between a charged pion in the calorimeter and the photon. Left: for Monte Carlo simulations. Right: for data. The black line indicates a cut which is used to reject split-off events. Events above that line are accepted.

chain.

The right panel of figure 2 right shows the missing mass deduced from two protons after particle identification in the forward detector. The  $\eta$ -peak is visible, along with background, from direct pion production.

In order to select  $\eta \rightarrow \pi^+ \pi^- \gamma$ -events, a least squares kinematic fit with constraint on the momentum and energy conservation was used. Events with a fit probability larger than 10% have been accepted. In addition to that, a cut on the photon energy and the opening angle between a pion and the photon has been implemented in the analysis of  $\eta \rightarrow \pi^+ \pi^- \gamma$  (see fig. 3). Pions cause hadronic split-offs in the calorimeter, which are reconstructed as low energetic photons (see fig. 3 left). This is the reason why the reaction  $pp \rightarrow pp \pi^+ \pi^-$  is the main background for  $\eta \rightarrow \pi^+ \pi^- \gamma$ .

$\eta \rightarrow \pi^+ \pi^- \pi^0$ -events are selected by using a kinematic fit with a constraint on energy and momentum conservation and the constraint  $\pi^0 \rightarrow \gamma \gamma$ . Events with a fit probability larger than 10% are accepted.

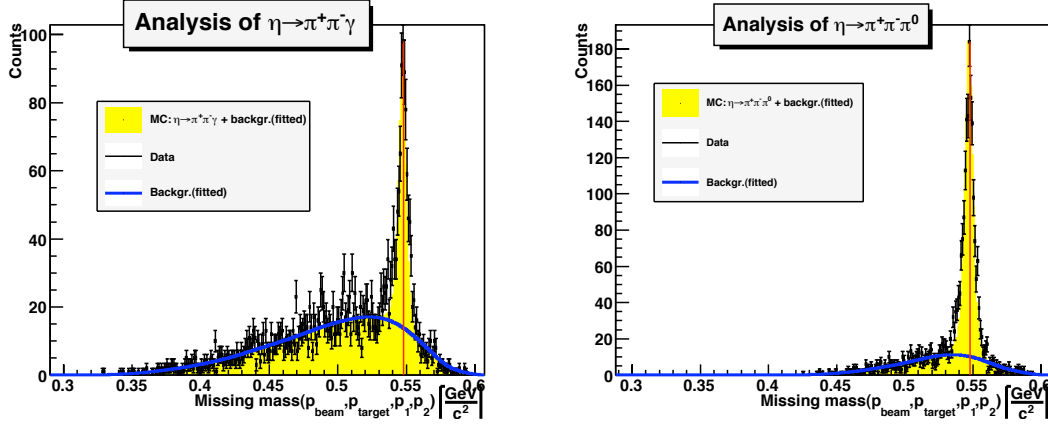


**Figure 4:** Left: Missing mass deduced from two protons for the analysis of  $\eta \rightarrow \pi^+ \pi^- \gamma$ . Right: Missing mass deduced from two protons for the analysis of  $\eta \rightarrow \pi^+ \pi^- \pi^0$ .

The results for analyzing  $\eta \rightarrow \pi^+ \pi^- \gamma$  are shown in the left part of fig. 4 left, as the results for analyzing  $\eta \rightarrow \pi^+ \pi^- \pi^0$  are shown in the right part of fig. 4. In both cases the background has been determined by using an iterative peak clipping algorithm (SNIP) (see blue curve in fig. /refresults). The results of both channels show a clear eta-signal in the missing mass spectrum after using a kinematic fit and suppressing split-off events. The comparison of simulation (see yellow shaded area in fig. /refresults) and data shows a good agreement.

### 3. Summary & outlook

After analyzing 1.2% of the total 2010 data, 703  $\eta \rightarrow \pi^+ \pi^- \gamma$  and 1,500  $\eta \rightarrow \pi^+ \pi^- \pi^0$ -events have been reconstructed by using a kinematic fit and a cut on hadronic split-off events in case of the analysis of  $\eta \rightarrow \pi^+ \pi^- \gamma$ . In a next step the relative branching ratio will be calculated and the single photon energy distribution for  $\eta \rightarrow \pi^+ \pi^- \gamma$  will be determined.

### Acknowledgements

This publication has been supported by the European Commission under the 7th Framework Programme through the ‘Research Infrastructures’ action of the ‘Capacities’ Programme. Call: FP7-INFRASTRUCTURES-2008-1, Grant Agreement N. 227431.

### References

- [1] Wess, Zumino, *Phys. Lett.*, **B37**, 95, (1971), Witten, *Nucl. Phys.*, **B223**, 422, (1983).
- [2] CLEO Collaboration, *Phys. Rev. Lett.*, **99**, 122001, (2007).
- [3] KLOE Collaboration, F.Ambrosio et al., arXiv:1107.5733 [hep-ex].
- [4] WASA Collaboration, P.Adlarson et al., *Phys. Lett.*, **B702**, 243-249 (2012).
- [5] F.Stollenwerk et al., *Phys. Lett.*, **B707**, 184-190 (2012).